Available online at www.sciencedirect.com
ScienceDirect
Journal of Hazardous Materials 152 (2008) 183–190
Journal of Hazardous Materials
www.elsevier.com/locate/jhazmat

Use of an integrated photocatalysis/hollow fiber microfiltration system for the removal of trichloroethylene in water

Kwang-Ho Choo [a,*], Dae-Ic Chang [a], Kyong-Won Park [b], Moon-Hyeon Kim [b]

[a] *Department of Environmental Engineering, Kyungpook National University, 1370 Sankyeok-Dong, Buk-Gu, Daegu 702-701, Republic of Korea*
[b] *Department of Environmental Engineering, Daegu University, 15 Naeri, Jillyang, Gyeongsan, Gyeongbuk 712-714, Republic of Korea*

Received 16 December 2006; received in revised form 12 May 2007; accepted 27 June 2007
Available online 6 July 2007

Abstract

This work focused on the degradation of toxic organic compounds such as trichloroethylene (TCE) in water, using a combined photocatalysis/microfiltration (MF) system. The performances of the hybrid system were investigated in terms of the removal efficiency of TCE and membrane permeability, in the presence or absence of background species, such as alkalinity and humic acids. The mass balancing of the fate of TCE during photocatalytic reactions was performed in order to evaluate the feasibility of the photocatalytic membrane reactor (PMR). Greater TCE degradation (>60%) was achieved with an increase in the TiO_2 dosage (up to 1.5 g/L) in PMR, but a substantially large TiO_2 dosage brought about a decrease in TCE degradation efficiency. The photocatalytic decomposition of TCE appeared to be more effective in acidic pH conditions than with a neutral or alkaline pH. The addition of alkalinity and humic acid into the feedwater did not have a significant effect on TCE degradation, while humic acids (whose dose was 1 mg/L as TOC) in the feedwater played a part in a decline of permeability by 60%. Membrane permeability in the PMR was also affected by tangential velocities. An improvement of 60% in flux was achieved when the tangential velocity increased from 0.19 to 1.45 m/s. This is because flow regimes can govern the deposition of TiO_2 particles on the membrane surface.

Keywords: Photocatalytic membrane reactor (PMR); Microfiltration; TiO_2; Trichloroethylene; Membrane fouling

1. Introduction

The occurrence of xenobiotic chemicals such as chlorinated organic compounds and pesticides in water sources has been great concerns to the public because of their toxicity [1,2]. For instance, trichloroethylene (TCE) is one of the widely used solvents in the chemical industry, and so the TCE contamination levels are in the range of a few hundreds ppm in wastewater down to a few ppb in groundwater [1,3]. The Korean acceptable level of TCE for the discharge of wastewater effluent is <0.3 mg/L and the guideline for drinking water is <0.03 mg/L. Several treatment methods for toxic organic chemicals would be available such as biological treatment [4,5], adsorption [6], ozonation [3], and catalytic oxidation [7]. Physiochemical approaches could be more reliable for the treatment of highly contaminated water compared to biological methods, which are limited due to the toxicity of the chemicals to microbes and the requirement of nutrients.

Currently, a photocatalytic degradation technique using TiO_2 is becoming increasingly popular for the removal of toxic and refractory organic compounds. This is because the photocatalytic method makes it possible for the organic compounds to be easily degraded under mild conditions [8–12]. The photocatalytic decomposition of many toxic organic contaminants such as cyanotoxin [13], humic substances [14,15], phenolic compounds [15], pesticides [16], endocrine disruptors [15], chlorinated compounds [15,17], and dyes [15] has been investigated with respect to the removal efficiency, reaction rate, and the formation of intermediates. Regarding organic pollutants, attempts have been made to decompose volatile organic compounds (VOCs) in a vapor phase rather than in an aqueous phase [18–20]. The vapor phase reaction, however, needs additional

* Corresponding author. Tel.: +82 53 950 7585; fax: +82 53 950 6579.
E-mail address: chookh@knu.ac.kr (K.-H. Choo).

0304-3894/$ – see front matter © 2007 Elsevier B.V. All rights reserved.
doi:10.1016/j.jhazmat.2007.06.117

treatment for the VOCs present in an aqueous phase such as air stripping, so that the direct, effective degradation of VOCs in water or wastewater would be more attractive with regard to the process design and operations.

The use of photocatalysts in various reactor configurations has been demonstrated in removing organic pollutants, such as fluidized beds [21], immobilized films [22–24], circulating columns [25], and membrane reactors [14,26–28]. The separation of photocatalysts after use, however, is another key issue that needs to be solved in terms of the practical applications of the process [29]. A major difficulty in the separation of TiO_2 particles from treated water arises because the particles are too fine to be removed by gravity settling. Other researchers have investigated the coagulation of fine catalysts or the attachment of TiO_2 particles onto a suitable substrate. In the former case, however, several further treatment steps are needed to recover the catalysts or the recovery is impractical [8]. In the latter case, the effective surface area of the TiO_2 particles would be reduced. In fact, it was reported that TiO_2 particles, while suspended, had a removal efficiency better than the immobilized ones [30]. Several studies regarding the use of membranes for the separation of TiO_2 particles have been conducted, but there were few reports on the application of loose, hollow fiber microfilters for the separation of the particles. Instead, tighter nano- and ultra-filtration technologies were employed while consuming more energy for the particle separation [14,15,20,31,32].

Therefore, the purpose of this work was to examine the performance of a photocatalytic reactor combined with hollow fiber microfiltration (MF) membranes for the degradation of a model toxic organic compound such as trichloroethylene (TCE) present in an aqueous phase. Mass balances were done to speculate the fate of TCE during photocatalytic reactions in the PMR. The effects of different operating conditions, such as TiO_2 doses, solution pH, and background compounds, on TCE removal efficiency were explored. Membrane permeability was also evaluated under different hydraulic conditions, during crossflow MF, concerning the separation of TiO_2 particles in the PMR.

2. Experimental

2.1. Feedwater and chemicals

A feed solution, containing TCE, was prepared by dissolving reagent-grade TCE (Janssen Chimica, Japan) in pure water prior to each experimental run. The TCE concentration was approximately 100 mg/L. To examine the effect of background species on the system efficiency, $NaHCO_3$ and $CaCl_2$ were added as inorganic species to adjust alkalinity and hardness to 50 mg/L as $CaCO_3$, respectively, while 1.0 mg total organic carbon (TOC) per liter of humic acids (Aldrich, USA) was added to the feedwater as a background organic compound. TiO_2 particles (P25, Degussa, Germany) were used as photocatalysts for the experiments and dosed in the range of 0–2.0 g/L. During photocatalysis, the reactor TiO_2 concentration was stable with stirring and continuous recirculation of the slurry through the hollow fiber module.

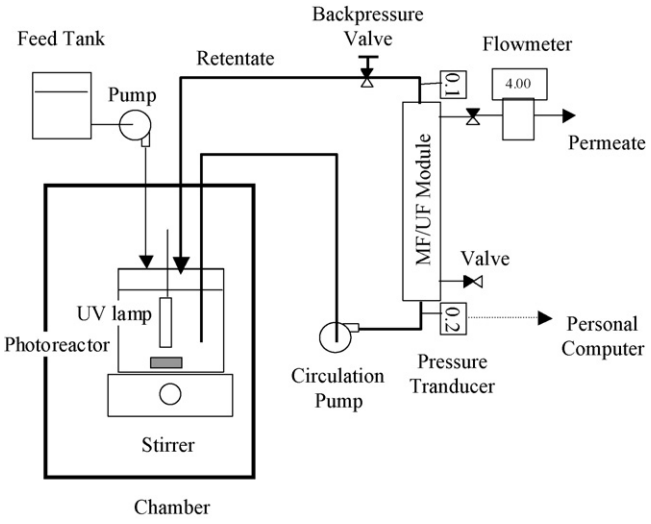

Fig. 1. A schematic of a lab-scale photocatalysis/MF system.

2.2. Photocatalytic membrane reactor operations

Fig. 1 shows a schematic diagram of the experimental setup, which is composed of a photocatalytic reactor and a crossflow MF module. The photocatalytic reactor had two main compartments, namely, an inner chamber and an outer chamber. A UV-light source was placed in the inner chamber of the reactor. The outer chamber can hold 700 mL of liquid for the photocatalytic reaction. The lab-scale MF module, holding three fibers, was prepared in the lab using polysulfone hollow fiber membranes supplied from SK Chemical, Korea. The hollow fiber membrane provided had a nominal pore size of 0.1 μm, an inner diameter of 700 μm, and its module with three fibers had an effective surface area of 20.7 cm^2 and a pure water permeability ranging from 146 to 219 L/(m^2 h) at 20 °C. There are a few advantages when three fibers are held in one lab-scale module. Firstly, having several fibers in a module is better than holding a single, long fiber in order to obtain the same surface area of a membrane due to the geometry of the PMR. Secondly, if a module holds a few fibers in it, the clogging of a fiber during MF could not cause a serious problem in obtaining permeate.

The hybrid PMR system was operated either in batch or continuous stirred tank reactor (CSTR) modes. In batch operations, the membrane permeate and retentate were recycled back to the photoreactor except for taking a minimal volume (∼20 mL) of permeate samples for analyses. In CSTR operations, the permeate was discharged to a sewer after taking samples as much as it was fed into the reactor. Thus the working volume of the reactor was maintained at a constant level of 700 mL. Although the MF system was designed to run under constant-pressure conditions, the system pressure and flux were monitored and recorded on an on-line personal computer in order to evaluate membrane permeability during MF in the PMR. The crossflow velocities inside the MF fibers were controlled in the range between 0.19 and 1.45 m/s (corresponding to 133–1015 in Reynolds number) by adjusting the circulation pump flow rate, while transmembrane pressure was regulated with a backpressure valve in order

Table 1
Summary of the experimental conditions and the portion of TCE classified

Condition	Process applied	TiO_2 dose (g/L)	UV lamp (W)	The portion of TCE classified
A	Vaporization	0	0	Remaining in the reactor; and vaporized
B	Adsorption and vaporization	1	0	Remaining in the reactor; vaporized; and adsorbed onto TiO_2
C	Photolysis and vaporization	0	8	Remaining in the reactor; vaporized; and degraded
D	Photolysis, adsorption, and vaporization	1	8	Remaining in the reactor; vaporized; adsorbed onto TiO_2; and degraded

to maintain the pressure level at 0.29 ± 0.01 bar. During photocatalysis, the TiO_2 suspension was irradiated using an 8-W black light blue UV-A lamp (Sankyo, Japan) with a maximum UV intensity at a wavelength of 365 nm. The temperature of water for batch and continuous processes varied in the range of 20–29 and 25–31 °C, respectively.

2.3. Mass balances on TCE

To analyze the fate of TCE in the PMR, mass balances on TCE were done conducting four sets of experiments under different operating conditions, which are summarized in Table 1. The following assumptions were made as we developed mass balances on TCE. Under condition A, the fate of TCE was classified into two categories: one was the TCE portion remaining in the reactor and the other was that vaporized. Under condition B, another portion considered was the TCE adsorbed onto TiO_2. The portion of TCE adsorbed was determined by subtracting the amount of TCE remaining in the reactor under condition B and that vaporized under condition A from the total TCE fed. Thus it was also assumed that the portion vaporized at condition B was the same as that at condition A. Under condition C, the TCE adsorbed is omitted, but the TCE that was degraded by photolysis was added while measuring the chloride (Cl^-) concentration in the reactor. The background Cl^- concentration was subtracted from the total chloride concentration measured in order to calculate the portion of TCE degraded. Condition D, where photocatalysis was occurring, included all the four categories of TCE. It was also assumed that the amount of TCE adsorbed was the same as that at condition B.

2.4. Analytical methods

The TCE and chloride ion concentrations in the reactor liquid and permeate were measured using a Shimadzu gas chromatograph (GC-17AATFw, Japan) equipped with a flame ionization detector and a Metrohm automatic titration system (702SM Tirtrino, Germany), respectively. The humic acids concentration was determined in terms of TOC using a Sievers TOC analyzer (Model 8200, USA) with a membrane conductivity detector. The pH and dissolved oxygen (DO) levels were monitored with a WTW InoLab system (Muti Level 3, Germany) and an Orion DO meter (Model 810, USA). The size distribution of TiO_2 particles in water was measured using a laser diffraction particle size analyzer (LS 13 320, Beckmann Coulter, USA). The TiO_2 concentrations were measured using an inductively coupled plasma spectrometer (Optima 2100 DV, Perkin-Elmer, USA). The photocatalytic products of TCE were identified using an Agilent gas chromatograph (model 6890N) equipped with a mass spectroscope (model 5795) detector (GC–MS).

3. Results and discussion

3.1. Photocatalysis and mass balancing of TCE during batch reactor operation

TCE removal efficiencies, during batch operations of the photocatalytic reactor, were evaluated in terms of the amounts of TCE removed and Cl^- ions produced, TOC removed in the aqueous phase (Fig. 2). The portion of TCE removed is based on the TCE remaining in a reactor, i.e., it equals to the total TCE fed minus the TCE remaining in the reactor. Thus, the TCE removed includes actual degradation, vaporization, and adsorption. The TCE degradation efficiency, based on the generation of Cl^- ions, was always maintained at a level lower than that based on the residual TCE concentration in the reactor. This could be attributed to the phenomena of vaporization and/or sorption of TCE during photocatalytic treatment. The formation of intermediates was also responsible for the difference between the values of TCE removed and Cl^- produced. The TOC remaining ($\sim$1 mg/L) in the reactor after 120-min photocatalysis exhibited the incomplete mineralization of TCE, which also indicated

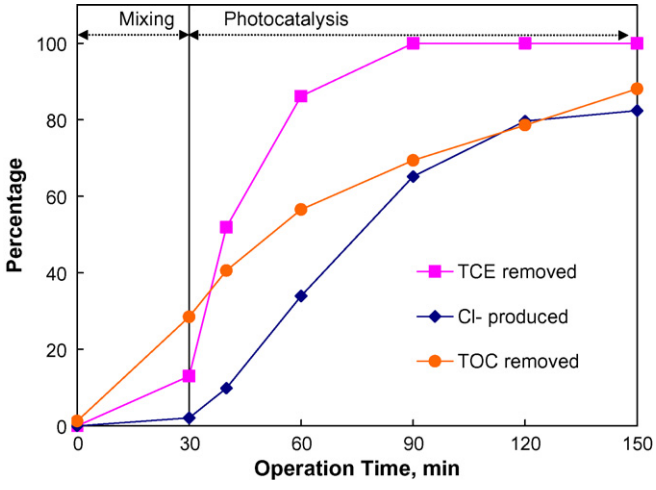

Fig. 2. Time course of TCE photocatalysis based on the TCE, Cl^-, and TOC concentrations. Photocatalysis started at 30 min after the solution was mixed: initial pH, 5.7; TiO_2 dose, 1.0 g/L.

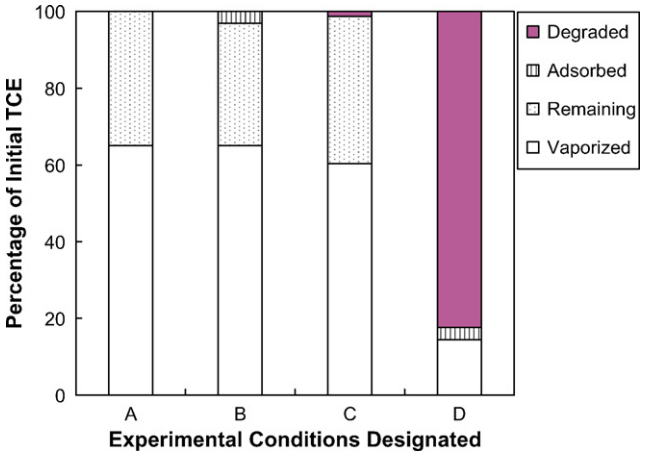

Fig. 3. Material balances on TCE at different experimental conditions. The conditions were designated based on TiO_2 dosage (in g/L) and UV-lamp status, respectively. (A) 0, off; (B) 1.0, off; (C) 0, on; (D) 1.0, on. Initial pH and reaction time for all tests was 5.3 ± 0.5 and 2 h, respectively.

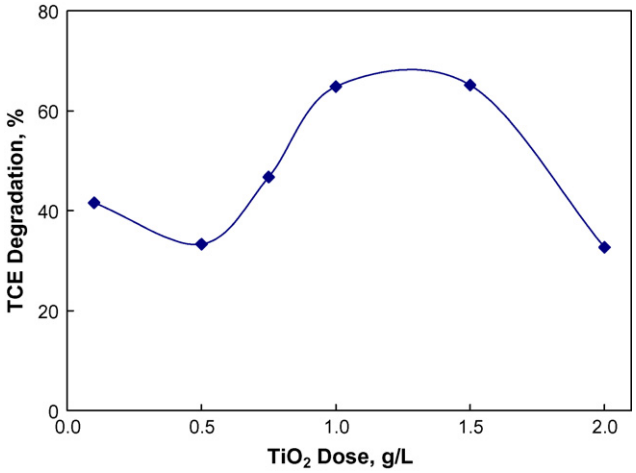

Fig. 4. Effects of TiO_2 dosage on TCE degradation efficiency: reaction time, 2 h; initial solution pH, 7.2 ± 0.3.

that some photocatalytic byproducts were formed. The identification of photocatalytic products of TCE will be discussed in subsequent section.

In order to determine the fate of TCE during photocatalytic reactions, mass balances on TCE were performed under different operating conditions and the results are shown in Fig. 3 (also refer to Table 1). A negligible amount of TCE was adsorbed on the surface of TiO_2 (experimental conditions A–D), whereas the amount of TCE vaporized was somewhat significant (approximately 65% at maximum), without the occurrence of photocatalytic reactions (experimental conditions A–C). TCE degradation by UV itself was minimal (1.25%) under condition C as reported elsewhere [13]. UV illumination, in the presence of TiO_2, contributed to substantial TCE degradation (82.4%), while at the same time causing a dramatic decrease in vaporization (condition D). This was probably because of the rapid conversion of TCE by photocatalysis. Consequently, the photocatalytic decomposition of TCE in water resulted in a significant reduction of TCE emission into the atmosphere as being mineralized or converted to less volatile intermediates.

3.2. Effects of TiO_2 doses and solution pH

Fig. 4 compares the ultimate TCE degradation efficiency at different TiO_2 dosages, in the PMR, after 2-h batch operations. When the TiO_2 dosage was changed in the range of 0.1–2.0 g/L, the TCE degradation efficiency reached its maximum at a TiO_2 concentration of 1.0–1.5 g/L. This implied that there was an optimal TiO_2 dosage for effective TCE removal, so a substantially large amount of TiO_2 in water might have an adverse effect. This is unclear, but a possible explanation is that it is caused by the scattering of UV-light by bare TiO_2 particles. Since TCE degradation reactions were supposed to occur on the surface of TiO_2 particles, photocatalysts that are not in contact with TCE would be interfering with UV-light illumination, thus leading to a decrease in the quantum yield of photoreactions.

The degradation efficiency of TCE by photocatalysis was also affected by the initial solution pH (Fig. 5), although the solution pH after 2-h reactions changed to ~3.0 for all the experiments tested, probably due to the generation of hydrogen chloride. The TCE degradation efficiency reached more than 80% at an acidic pH level, while it decreased to approximately 60–65% at a neutral and alkaline pH region. Based on the findings reported elsewhere [10,18,33], the heterogeneous photocatalytic initiation (reactions (1)–(5)) and the proposed reductive degradation pathways (reactions (6)–(9)) are listed below:

$$TiO_2 + h\nu \rightarrow h^+_{vb} + e^-_{cb} \quad (1)$$

$$h^+_{vb} + OH^- \rightarrow {}^\bullet OH \quad (2)$$

$$e^-_{cb} + O_2 \rightarrow O_2{}^\bullet \quad (3)$$

$$O_2{}^\bullet + e^-_{cb} + H^+ \rightarrow H_2O_2 \quad (4)$$

$$H_2O_2 + e^-_{cb} \rightarrow {}^\bullet OH + OH^- \quad (5)$$

$$CHCl{=}CCl_2 + e^-_{cb} \rightarrow [CHCl{=}CCl_2{}^\bullet]^- \quad (6)$$

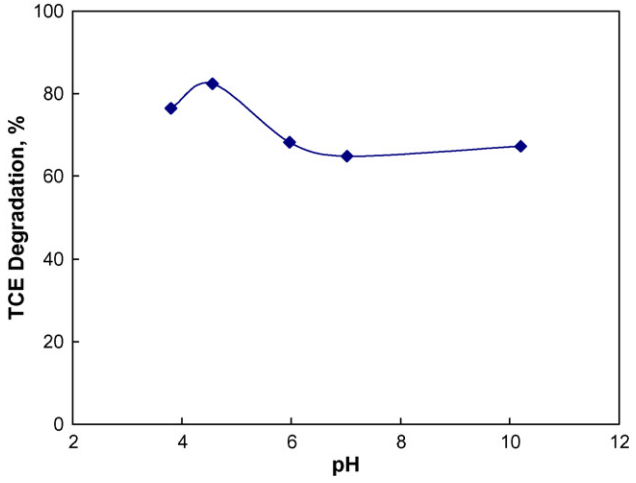

Fig. 5. Effects of initial solution pH values on the TCE degradation efficiency: TiO_2 dose, 1.0 g/L; reaction time, 2 h.

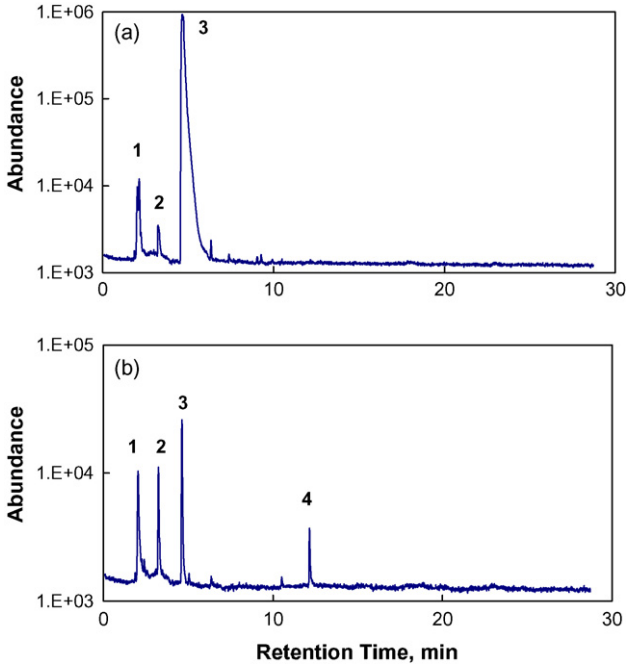

Fig. 6. The GC–MS analyses of photocatalytic products of TCE at: (a) reaction time of 10 min and (b) reaction time of 90 min. The peaks were identified as follows: (1) carbon dioxide; (2) chloroform; (3) TCE; and (4) pentachloroethane.

$$[CHCl{=}CCl_2{}^{\bullet}]^- + H^+ \rightarrow {}^{\bullet}CHCl{-}CHCl_2 \quad (7)$$

$$CHCl{=}CCl_2 + O_2{}^{\bullet -} \rightarrow CHCl(O_2{}^{\bullet -}){-}CCl_2 \quad (8)$$

$$CHCl(O_2{}^{\bullet -}){-}CCl_2 + H^+ \rightarrow CHCl(O_2{}^{\bullet}){-}CHCl_2 \quad (9)$$

This may suggest that reductive reaction pathways would be more responsible for the decomposition of TCE while interacting with the TiO_2 conduction band electrons (e_{cb}^-) and anion superoxide radicals ($O_2{}^{\bullet -}$) under an acidic pH. The generation of hydroxyl radicals (reaction (5)), the reductive destruction of vinyl groups in TCE (reactions (6) and (7)), and the direct attack of superoxide anion radicals to TCE (reactions (8) and (9)) appeared to be favored under acidic conditions.

In addition, the three major photocatalytic products of TCE such as carbon dioxide, chloroform, and pentachloroethane were identified by GC–MS (Fig. 6). Their formation was more obvious at reaction time of 90 min. However, we were not able to detect phosgene and dichloroacetic chloride, which was reported in the other findings [17,33]. Two possible reaction pathways during the TiO_2 photocatalytic degradation of TCE were proposed [33]. The products of the chlorination route such as chloroform and pentachloroethane were only detected in this work, suggesting that route would be the major path during PMR treatment.

3.3. TCE degradation during continuous-flow reactor operation

Fig. 7 shows the variation of TCE degradation efficiency and solution pH during PMR operations when additional background species were present in feedwater. In the calculation of the TCE degradation based on the Cl^- concentration produced

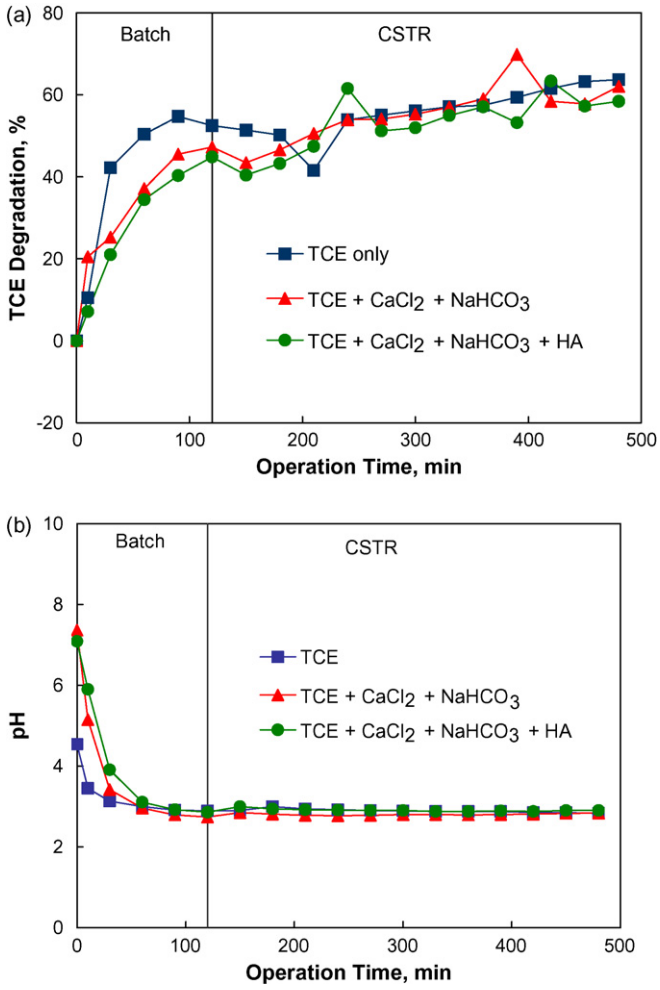

Fig. 7. Variation of (a) TCE degradation efficiency and (b) pH with time during batch and CSTR operations: TiO_2 dosage, 1.0 g/L; retention time in CSTR, 150 min. The reactor was initially operated in a batch mode and then switched to CSTR operation after 120 min.

during photocatalysis, the background chloride concentration was subtracted from the total chloride concentration measured. The TCE degradation efficiency increased up to >40% during the initial 120-min batch operation, and it kept increasing during the CSTR operation of the PMR with a hydraulic retention time of 150 min. An increased TCE degradation in the batch mode is related to the initial pH of feedwater as shown in Fig. 7b, but it is also possible that TCE degradation may proceed relatively slowly with the addition of the background components such as bicarbonate. This might be attributed to the scavenging effect of hydroxyl or anion superoxide radicals by alkalinity [10].

$$HCO_3{}^- + {}^{\bullet}OH \rightarrow CO_3{}^{\bullet -} + H_2O \quad (10)$$

$$CO_3{}^{2-} + {}^{\bullet}OH \rightarrow CO_3{}^{\bullet -} + OH^- \quad (11)$$

On the other hand, humic acids might enhance the photocatalytic degradation of chlorinated compounds such as TCE because they could serve as a hole (h_{vb}^+) scavenger improving its reductive degradation [18]. When the photocatalysis of a solution containing humic acids alone of ~1.0 mg/L as TOC was conducted in this work, the TOC concentration decreased

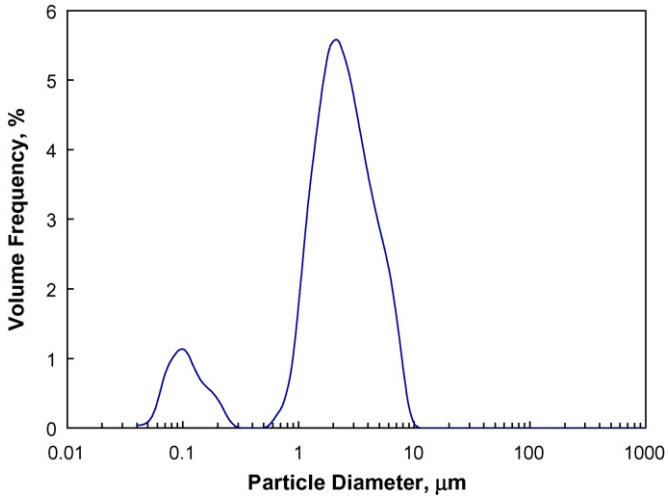

Fig. 8. The size distribution of the TiO_2 particles added to the feedwater.

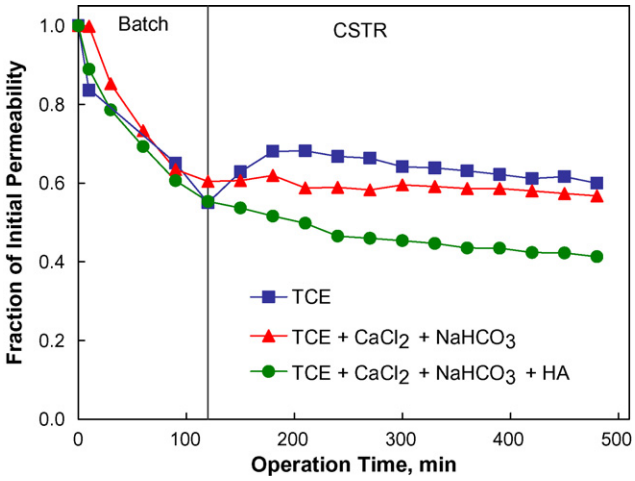

Fig. 9. Membrane permeability vs. time during batch and CSTR operations: tangential velocity, 1.45 m/s; initial water permeability, 188–219 L/(m^2 h).

sharply down to 0.058 mg/L within 240-min PMR operation (data not shown). A substantial amount of humic acids (>92%) were removed by photocatalytic membrane treatment. The humic acids, however, did not seem to affect the photocatalysis of TCE significantly. A possible explanation for the result is: the humic acids become attached to the TiO_2 surface and so act as a hole scavenger; however, they also can occupy the active sites of TiO_2 for the photoreaction of TCE while interfering with TCE degradation. The presence of humic acids had both their pros and cons regarding the photocatalytic degradation of TCE, which stroke a balance showing no marked improvement in the TCE removal efficiency. Further studies on TCE degradation in the presence of humic acids are needed. Overall, the TCE degradation proceeded stably in continuous PMR operations. The influence of background components such as hardness (Ca^{2+}), alkalinity, and humic acids on TCE degradation was found negligible in CSTR since solution pH was maintained at ~3 and so no bicarbonate ions ($pK_a = 6.4$) existed any more.

3.4. TiO_2 separation and membrane permeability in PMR

The complete separation of TiO_2 particles from treated water (turbidity of permeate < 0.1 NTU) was possible during continuous operations of PMR with hollow fiber MF membranes. Although the sizes of the TiO_2 particle grains in water were between 0.04 and 10 μm in diameter, the majority of particles was >0.4 μm (Fig. 8), so they can be rejected by the MF membrane. The other portions of TiO_2 particles that were in the range of the sizes smaller than the size of membrane pores (0.1 μm) might have a chance to pass through the membrane. In reality, however, the measured TiO_2 concentration in the permeate sample was nearly negligible (<0.5 ppb). This was because during MF in the PMR, the big TiO_2 particles could form a dense cake layer (which is called "secondary dynamic membrane") on top of the actual membrane, which would help further reject the smaller particles. This also confirms that the use of a hollow fiber MF membrane would be reliable for the enhanced performance of photocatalysis while maximizing the capacity of suspended photocatalysts in the PMR.

As shown in Fig. 9, however, a sharp decline in membrane permeability was observed when humic acids were present in feedwater. This was due to the sorption of humic acids onto TiO_2 particles and their subsequent deposition on the membrane surface, thus leading to membrane fouling [14]. The reduction of permeability was significant when the crossflow velocity decreased from 1.45 to 0.19 m/s (Fig. 10). It could be hypothesized that the accumulation of humic acid-laden TiO_2 particles on the membrane surface may cause such a significant permeability reduction. In order to examine the significance of TiO_2 deposition, MF with UV illumination was performed using a single-component system containing either TCE or TiO_2 (Fig. 11). There was no indication of membrane fouling by TCE itself, but the TiO_2 particles brought about a substantial decline in permeability at a low tangential velocity. As a result, it was necessary to maintain a higher tangential velocity across the membrane surface in order to minimize membrane fouling, which was caused by TiO_2 deposition in the PMR.

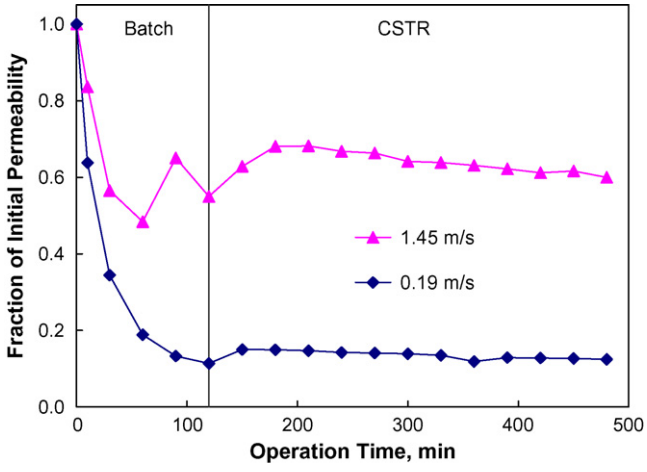

Fig. 10. Effects of tangential velocity on membrane permeability during crossflow MF: initial water permeability, 183–219 L/(m^2 h).

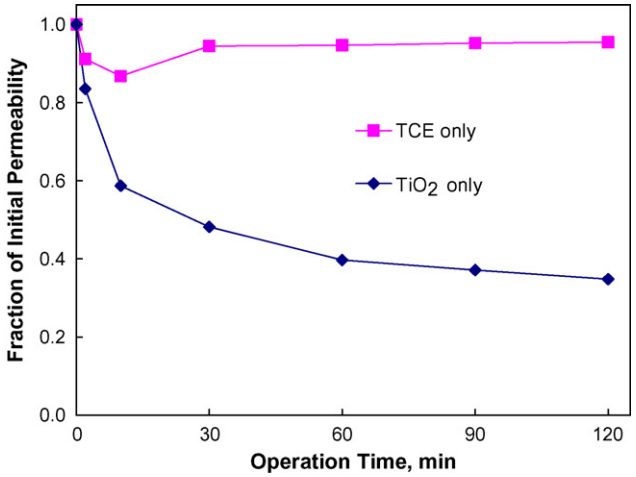

Fig. 11. A comparison of membrane permeability with a single-component system containing TCE or TiO_2 alone in liquid: tangential velocity, 0.19 m/s; initial water permeability, 146–194 L/(m^2 h).

4. Conclusions

The coupling of TiO_2 photocatalysts and crossflow MF membranes was investigated regarding the degrading of TCE in water, during batch and CSTR operations. The effects of the TiO_2 dosage, solution pH, and background species on TCE removal was examined along with the mass balancing of TCE degradation in the PMR. Membrane permeability was also evaluated using feed solutions containing various background components at different tangential velocities. The following conclusions can be drawn:

(1) Substantial TCE degradation (>60%) was achieved within 2 h by continuous photocatalysis/MF, which can contribute to the significant decrease of TCE vaporization from water to air through either the mineralization or conversion of TCE to less volatile products.
(2) TCE degradation in the PMR was maximal with a photocatalyst dosage of 1.0–1.5 g/L, since too low or high dosages of TiO_2 could be related to either the lack of surface area for reactions or the blocking of UV-light irradiation. The photocatalytic degradation of TCE was more effective at an acidic pH than at a neutral or alkaline pH, indicating that reductive pathways involved play a more important role in TCE degradation.
(3) Alkalinity might retard TCE decomposition due to its scavenging of hydroxide or anion superoxide radicals, but the TCE degradation in continuous PMR operations was not affected by the background species present because the solution pH became acidic (pH ∼ 3).
(4) Although photocatalysis, followed by crossflow MF, was effective for the complete separation of TiO_2 particles in suspension from treated water, higher tangential velocity was needed to control membrane fouling caused by the deposition of humic acid-laden TiO_2 on the membrane surface.

Acknowledgements

This work was supported by the Korea Science and Engineering Foundation (Grant R01-2002-000-00524-0). The authors thank Mr. Won-Young Ahn of Kolon Engineering and Construction Co. for his help in obtaining hollow fiber MF membranes. We extend our appreciation to SK Chemical for hollow fiber membranes.

References

[1] R.E. Watson, C.F. Jacobson, A.L. Williams, W.B. Howard, J.M. DeSesso, Trichloroethylene-contaminated drinking water and congenital heart defects: a critical analysis of the literature, Reprod. Toxicol. 21 (2006) 117–147.
[2] M. Gutiérrez, J. Etxebarria, L. de las Fuentes, Evaluation of wastewater toxicity: comparative study between Microtox® and activated sludge oxygen uptake inhibition, Water Res. 36 (2002) 919–924.
[3] B. Battacharyya, T.F. Van Dierdonck, S.D. West, A.R. Freshour, Two-phase ozonation of chlorinated organics, J. Hazard. Mater. 41 (1995) 73–93.
[4] C. Misra, S.K. Gupta, Hybrid reactor for priority pollutant-trichloroethylene removal, Water Res. 35 (2001) 160–166.
[5] B. Tartakovsky, M.F. Manuel, S.R. Guiot, Degradation of trichloroethylene in a coupled-aerobic bioreactor: modeling and experiment, Biochem. Eng. J. 26 (2005) 72–81.
[6] P.A. Quinlivan, L. Li, D.R.U. Knappe, Effects of activated carbon characteristics on the simultaneous adsorption of aqueous organic micropollutants and natural organic matter, Water Res. 39 (2005) 1663–1673.
[7] M.H. Kim, K.H. Choo, Low-temperature continuous wet oxidation of trichloroethylene over CoO_x/TiO_2 catalysts, Catal. Commun. 8 (2007) 462–466.
[8] S. Kagaya, K. Shimizu, R. Arai, K. Hasegawa, Separation of titanium dioxide photocatalyst in its aqueous suspensions by coagulation with basic aluminum chloride, Water Res. 33 (1999) 1753–1755.
[9] D.D. Dionysiou, M.T. Suidan, E. Bekou, I. Baudin, J.M. Laîné, Effect of ionic strength and hydrogen peroxide on the photocatalytic degradation of 4-chlorobenzoic acids in water, Appl. Catal. B 26 (2000) 153–171.
[10] K. Pirkanniemi, M. Sillanpää, Heterogeneous water phase catalysis as an environmental application: a review, Chemosphere 48 (2002) 1047–1060.
[11] Z. Ai, P. Yang, S. Lu, Degradation of 4-chlorophenol by a microwave assisted photocatalysis method, J. Hazard. Mater. B 124 (2005) 147–152.
[12] R.H. Kim, S. Lee, Y.M. Kim, J.H. Lee, Pollutants in rainwater runoff and their control by surface modification using TiO_2, J. Ind. Eng. Chem. 10 (2004) 152–160.
[13] P.J. Senogles, J.A. Scott, G. Shaw, H. Stratton, Photocatalytic degradation of the cyanotoxin cylindrospermopsin using titanium dioxide and UV irradiation, Water Res. 35 (2001) 1245–1255.
[14] S.A. Lee, K.H. Choo, C.H. Lee, H.I. Lee, T. Hyeon, W. Choi, H.H. Kwon, Use of ultrafiltration membranes for the separation of TiO_2 photocatalysts in drinking water treatment, Ind. Eng. Chem. Res. 40 (2001) 1712–1719.
[15] R. Molinari, M. Borgese, E. Drioli, L. Palmisano, M. Schiavello, Hybrid processes coupling photocatalysis and membranes for degradation of organic pollutants in water, Catal. Today 75 (2002) 77–85.
[16] M. Munner, M. Qamar, M. Saquib, D.W. Bahnemann, Heterogeneous photocatalysed reaction of three selected pesticide derivatives, propham, propachlor and tebuthiuron in aqueous suspensions of titanium dioxide, Chemosphere 61 (2005) 457–468.
[17] S.K. Joung, T. Amemiya, M. Murabayashi, K. Itoh, Adsorbed species on TiO_2 associated with the photocatalytic oxidation of trichloroethylene under UV, J. Photochem. Photobiol. A: Chem. 183 (2006) 273–281.
[18] E. Selli, D. Baglio, L. Montanarella, G. Bidoglio, Role of humic acids in the TiO_2-photocatalyzed degradation of tetrachloroethene in water, Water Res. 33 (1999) 1827–1836.
[19] P.B. Amama, K. Itoh, M. Murabayashi, Photocatalytic oxidation of trichloroethylene in humidified atmosphere, J. Mol. Catal. A: Chem. 176 (2001) 165–172.

[20] Z. Guo-Min, C. Zhen-Xing, X. Min, Q. Xian-Qing, Study on the gas-phase photolytic and photocatalytic oxidation of trichloroethylene, J. Photochem. Photobiol. A: Chem. 161 (2003) 51–56.
[21] T.H. Lim, S.D. Kim, Trichloroethylene degradation by photocatalysis in annular flow and annulus fluidized bed photoreactors, Chemosphere 54 (2004) 305–312.
[22] S.C. Ryu, M.S. Kim, B.W. Kim, Photodegradation of alachlor with the TiO_2 film immobilized on the glass tube in aqueous solution, Chemosphere 53 (2003) 765–771.
[23] M.S. Lee, J.D. Lee, S.S. Hong, Photocatalytic decomposition of acetic acid over TiO_2 and TiO_2/SiO_2 thin films prepared by the sol–gel method, J. Ind. Eng. Chem. 11 (2005) 495–501.
[24] A. Bouzaza, C. Vallet, A. Laplanche, Photocatalytic degradation of some VOCs in the gas phase using an annular flow reactor: determination of the contribution of mass transfer and chemical reaction steps in the photodegradation process, J. Photochem. Photobiol. A: Chem. 177 (2006) 212–217.
[25] J.H. Jeon, S.D. Kim, T.H. Lim, D.H. Lee, Degradation of trichloroethylene by photocatalysis in an internally circulating slurry bubble column reactor, Chemosphere 60 (2005) 1162–1168.
[26] J. Ryu, W. Choi, K.H. Choo, A pilot-scale photocatalyst-membrane hybrid reactor: performance and characterization, Water Sci. Technol. 51 (2005) 491–497.
[27] P. Le-Clech, E.K. Lee, V. Chen, Hybrid photocatalysis/membrane treatment for surface waters containing low concentrations of natural organic matters, Water Res. 40 (2006) 323–330.
[28] R. Molinari, L. Palmisano, E. Drioli, M. Schiavello, Studies on various reactor configurations for coupling photocatalysis and membrane process in water purification, J. Membr. Sci. 206 (2002) 399–415.
[29] K. Tennakone, C.T.K. Tilakaratne, I.R.M. Kottegoda, Photocatalytic degradation of organic contaminants in water with TiO_2 supported on polythene films, J. Photochem. Photobiol. A: Chem. 87 (1995) 177–179.
[30] D. Robert, A. Gauthier, Prospects for a supported photocatalyst in the detoxification of drinking water, Water Qual. Int. (November/December) (1998) 27.
[31] K. Sopajaree, S.A. Qasim, S. Basak, K. Rajeshwar, An integrated flow reactor-membrane filtration system for heterogeneous photocatalysis. Part I: experiments and modeling of a batch recirculated photoreactor, J. Appl. Electrochem. 29 (1999) 533–539.
[32] S. Mozia, M. Tomaszewska, A.W. Morawski, Removal of azo-dye Acid Red 18 in two hybrid membrane systems employing a photodegradation process, Desalination 198 (2006) 183–190.
[33] K.H. Wang, J.M. Jehng, Y.H. Hsiech, C.Y. Chang, The reaction pathway for the heterogeneous photocatalysis of trichloroethylene in gas phase, J. Hazard. Mater. B 90 (2002) 63–75.